Mat. Res. Soc. Symp. Proc. Vol. 731 © 2002 Materials Research Society

A Model for Comprehensive Studies of Porosity in Mesoporous Low-K Dielectrics

Mihail P. Petkov
Jet Propulsion Laboratory, California Institute of Technology,
4800 Oak Grove Drive, Pasadena, CA 91109, U.S.A.

ABSTRACT

The successful integration of a porous low dielectric constant (k) material as an interlevel dielectric depends on the morphology of the embedded porosity. Simple site percolation models are utilized here to investigate porosity properties of low-k dielectrics with respect to the current technology trends. Significant differences between two generations of porous dielectrics, $k < 2.4$ and $k < 2.1$, are found. The porosity fraction in the latter is above the percolation threshold, which may have serious impact on the materials physical properties and its compatibility with production steps.

INTRODUCTION

Historically, the performance of electronic devices has been improved by miniaturizing the devices, which lowered the transistor gate delays. However, the signal propagation delay (*RC* delay; *R* – metal resistance, *C* – dielectric capacitance) became the dominant factor to-date, and future advances rely on overcoming the materials limitations. For this end, Cu instead of Al interconnects are already used in state-of-the-art devices, and low dielectric constant (low-k, $k < 2.7$) materials are sought to substitute the SiO_2 as interlevel dielectrics (ILD's). Companies are adopting different strategies for this transition; however, most of them will use low-k dielectrics for the 0.13 μm node [1]. Next-generation technologies will require ultra-low-k ILD's with effective $k < 2.1$, which must incorporate porosity ($k \approx 1$). Manufacturable ultra-low-k solutions are not presently known [2].

The integration of the low-k materials faces many problems [1]. In comparison with SiO_2, lower k values are achieved at the expense of a spectrum of other properties, such as hardness, strength, thermal conductivity, adhesion, metal diffusion, etc. They will be further compromised by the presence of porosity, and the compatibility with some production steps will be severely degraded. Thus, understanding the role of the porosity morphology on the characteristics of the materials is important for the successful integration of any low-k material as ILD.

Computer-based models built on percolation theory [3-5] are especially suitable for studies of porous materials. They have been successfully utilized in diverse areas, such as micro-fluidics, selective catalysis, molecular separation, chemical sensing, electro-optics, and microelectronics. In this work, simple models are utilized in a qualitative investigation of the relationship between the morphology of the porosity and the technology requirements given in the *International Technology Roadmap for Semiconductors* (*ITRS*) [2].

PERCOLATION MODELS

A square lattice site percolation is considered here as an example of a two-dimensional (2D) percolation model. A pore occupies a site in a $L \times L$ square cell with a probability p ($0 \le p \le 1$). If two adjacent sites are occupied, the respective pores are considered connected, e.g., allowing an imaginary particle to percolate from one pore to the other. All accessible pores to an imaginary particle placed in a given pore form a cluster. Clusters grow in size with the increase of porosity. At some critical value of p, denoted as percolation threshold, p_c, an infinite cluster is formed. In the finite-scale computer model, this is represented by the creation of a pathway through connected pores, spanning across the cell. This phenomenon, which is one of the main subjects studied by the percolation theory, represents a first order phase transition.

An analogous three-dimensional (3D) site percolation model on a simple cubic lattice ($L \times L \times L$) is also considered here. $L = 1000$ for the 2D and $L = 100$ for the 3D cells were chosen as a compromise for obtaining a reasonable accuracy without using an excessive amount of computer time. Precise calculations of the respective percolation thresholds lie outside of the scope of this work. Their values are known with high accuracy: $p_c(2D) = 0.592746$ and $p_c(3D) = 0.311600$ [6]. The 2D and 3D models have many similar qualities. An important difference is the coexistence of two continuous phases (solid and open) for $p_c < p < (1 - p_c)$ in the 3D case.

In both models, the clusters were separated into two groups: isolated clusters, which do not contain a percolation path to any of the surfaces, and open clusters, which extend to at least one side of the cell. The ratio of the sum mass (number of occupied sites) of all open clusters and the sum mass of all pores defines the open porosity fraction, F_{open}. F_{open} is a suitable parameter to demonstrate percolation effects, and a comparison with p_c is used here for model validation. For calibration purposes, F_{open} is calculated per side. Care is taken to avoid multiple counting of non-percolation open clusters, which reside on two or more surfaces. Although this expression does not affect p_c, the comparison with the analytical result that F_{open} approaches $1/L$ for $p \to 0$ provides a useful calibration. Calculated also is the density of the isolated clusters, defined as number of clusters per unit volume (cell volume: L^2 in 2D; L^3 in 3D). These results are nearly independent on the cell size for a sufficiently large cell. The density of single pores, multiple-pore clusters and all isolated clusters are monitored separately as a function of p.

The results are presented as a function of the *loading probability*, p, which is sometimes referred to as *number density* (n). The *reduced number density*, η, (or *volume fraction*) is the more appropriate parameter when actual pore shapes are considered. The relationship between η and n is $\eta = n \times f$, where f is the *filling factor*, representing the available volume in which pores can be placed.

As an example, consider disks with a diameter $d = 1$ (the spacing between neighbor sites) in the 2D square model (Figure 1). When two neighbor sites are occupied (Figure 1, solid disks), the two disks touch in one point, through which a percolation path can pass. In such an

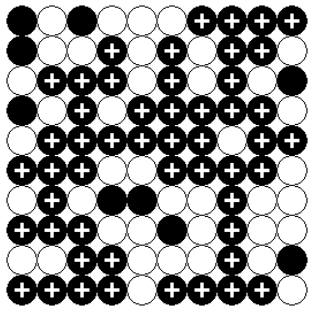

Figure 1. A representation of a 2D site percolation model on a square lattice with disk-like shaped pores (black). Sites are filled randomly with $p = 0.6$ ($p_c \approx 0.593$) and the pores, which belong to the percolation cluster, are marked with a "+" sign.

arrangement, when all sites are occupied ($p = 1$) a part of the cell area is inaccessible to the disks (no disk can be placed there). Therefore, the available volume fraction is $f = \pi/4 \approx 0.7854$, and percolation, using the values from Ref. [6], occurs at $\eta_c = 0.465542$. An analogical example for 3D considers spheres with $d = 1$, which gives $f = \pi/6 \approx 0.5236$ and $\eta_c = 0.163153$.

The use of an adequate model for representing the subject is critical for obtaining valid quantitative results. However, it has been demonstrated that the reduced number density carries little model dependence for disks (2D) and spheres (3D) [7]. The present study sets the stage for future improved representations of the porous dielectrics perhaps utilizing the Bernal model for randomly packed hard spheres [8]. An even more realistic scenario is to enable the pores to coordinate on a distance larger than 1 (beyond the nearest neighbors) [9,10]. Inherent features to the low-k production method may require a careful treatment of the interactions, which may shift the percolation threshold to either higher or lower values [11]. Other models, considering pores comprised of a hard core and a soft shell [12], may also be suitable.

The program code used here was written in a Matlab environment, and the calculations were done on a 1 GHz personal computer with 512 Mb memory. The code utilizes a number of functions specifically designed for Matlab for image analysis applications. Their utilization enables this preliminary research on reasonably large cells without the use of a supercomputer.

RESULTS

Figure 2 shows the open porosity fraction, F_{open}, as a function of p for the 2D (Figure 2(a)) and 3D models (Figure 2(b)). The top scales show the reduced number density, η_c, using the filling factors for disks and spheres, respectively. The percolation thresholds for both cases, whose values are adopted from Ref. [6], are shown with vertical lines.

The good agreement between the onset for the open porosity increase and the p_c values is evident. In their vast majority, the efforts of modeling percolation phenomena are focused on the details with which this phase transition occurs. For this study, however, more attention is directed towards the low values of p for reasons, which will become clear below.

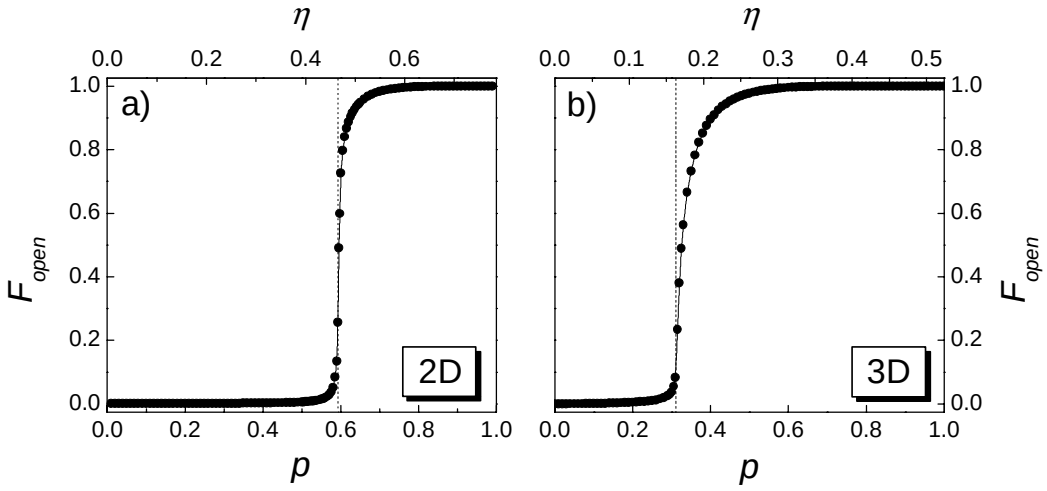

Figure 2. Open porosity fraction of site percolation models: **(a)** two-dimensional on a square lattice; **(b)** three-dimensional on a cubic lattice. The respective percolation thresholds $p_c = 0.592746$ (2D) and $p_c = 0.311600$ (3D) are shown with vertical lines. The top scales give the reduced number densities for disks and spheres, respectively.

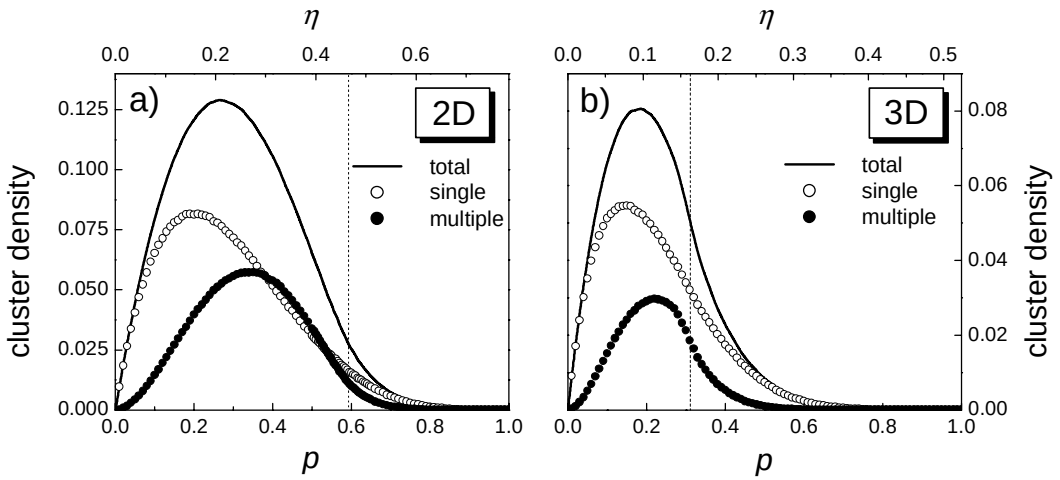

Figure 3. Densities of isolated clusters in site percolation models: **(a)** two-dimensional on a square lattice; **(b)** three-dimensional on a cubic lattice. Shown are the total density (solid line), and the densities of single pores (open symbols), and multiple-pore clusters (solid symbols). As in Figure 2, the respective percolation thresholds are marked with vertical lines, and the top scale shows the respective reduced number densities for disks (2D) and spheres (3D).

The cluster density results from the 2D and 3D models are presented in Figure 3(a) and 3(b), respectively. The vertical lines mark the percolation thresholds in the two cases. Identical symbols are used to represent the corresponding data in both sub-plots: solid line for the total isolated cluster density, open circles for the density of single pores, and solid circles for the multiple-pore cluster density.

DISCUSSION

A meaningful dielectric constant of the considered solid must be assumed in order to relate the present results to porous low-*k* dielectrics and investigate their properties against the guidelines given in the *ITRS* [2]. A realistic approach requires the consideration of existing low-*k* materials with high commercialization potentials. One such material is SiLK™, because of its successful integration with Cu metallization schemes [13]. The dielectric constant of SiLK™ is 2.65. Another material worth considering is methyl-silsesquioxane (MSSQ), whose dielectric constant ranges between 2.7 and 2.85. A number of other non-porous spin-on materials also exhibit dielectric constants in the 2.6–2.9 range. Compositionally similar to MSSQ materials (SiCOH) with dielectric constant in this range have also been produced by chemical vapor deposition. Therefore, the assumption of k_0 = 2.7-2.8 is in a reasonable range.

A simple superposition model can be considered to calculate the amount of required embedded porosity, with which a given preset *k*-value will be achieved. The porous dielectric can be represented by two slabs – one, consisting of the compressed solid material without the porosity with dielectric constant k_0, and a layer of air ($k \approx 1$) with volume equal to that of the initial porosity ("projected" porosity). The film thickness remains unchanged. Being area-independent, the thickness ratio of the air-slab and the whole film is equal to the porosity volume

fraction, η. The effective dielectric constant, k_{eff}, is then equivalent to that of two capacitors connected in series, each with the thickness and dielectric constant of the respective slabs. Thus, to achieve a dielectric constant of k_{eff} ($k_{eff} < k_0$), x is calculated as follows:

$$\eta = \frac{k_0 - k_{eff}}{(k_0 - 1) \cdot k_{eff}} . \quad (1)$$

This approach is known to be successful in representing porous materials, and has been utilized to calculate foaming efficiencies of volatile polymers [14], which were used to produce porous MSSQ films [15] in a wide porosity range. Thus, we can calculate the porosity fractions in low-*k* materials, necessary to reproduce the development trends underlined by the *ITRS*. Given in *Table I* are the values of the effective dielectric constant (due to low-*k* and etch-stop layers) and the requirements for the bulk low-*k* values. The bold numbers denote known manufacturable solutions; the unknown manufacturable solutions are shown with bold-underlined numbers.

Thus, values of $k = 2.4$ can be achieved (with $k_0 = 2.7–2.8$) with 7–9% porosity, whereas $k = 2.1$ requires 17–19% porosity. A close inspection of Figure 2(b) in this context indicates a drastic difference in the properties of these two examples – the porosity load in the latter material is above the percolation threshold. (It should be remembered that this result carries little model dependency [7]). A porous material with porosity above the percolation threshold has many drawbacks. The significant changes in mechanical strength and hardness may compromise its integration and may degrade its compatibility with processes such as chemical-mechanical polishing. Metal diffusion is strongly enhanced in a porous media. Alterations of reactive ion etch steps may occur due to the increased accessible surface area. The damascene metallization process may result in Cu lines with irregular geometry. The formation probability of a "killer pore", which when filled with Cu during metallization shorts neighboring wires, increases abruptly above the percolation threshold; any part of the percolation cluster may form a "killer pore". Therefore, apart from the gradual porosity increase, sharp changes in other properties can give rise to major technologically important challenges in the transition from the $k = 2.4$ to 2.1.

In contrast to $k = 2.1$, the porosity in the $k = 2.4$ dielectric appears to be optimized in terms of pore connectivity. The ~9% porosity in the solid with $k \sim 2.8$ is comprised mostly of isolated clusters, whose density is at its maximum. Moreover, the $k \sim 2.7$ material needs ~7% porosity, at which the single pore density is maximized, and thus minimum surface roughness is obtained. This is preferable at identical other properties, since such morphology will benefit a number of production steps.

Table I. Extracts from ITRS [2]: the effective and bulk dielectric constants in microprocessor (MPU) technology. Bold text: manufacturable solutions exist; bold-underlined text: manufacturable solutions not presently known.

Year of production	2001	2002	2003	2004	2005	2006	2007
MPU: Interlevel metal insulator – effective dielectric constant (k)	3.0-3.6	3.0-3.6	3.0-3.6	**2.6-3.1**	**2.6-3.1**	**2.6-3.1**	**2.3-2.7**
MPU: Interlevel metal insulator – bulk dielectric constant (k)	< 2.7	< 2.7	<2.7	**< 2.4**	**< 2.4**	**< 2.4**	**< 2.1**

CONCLUSIONS

This feasibility study utilizes percolation models to explore the connection between the low-*k* development guidelines given in the *ITRS* and the porosity morphology in low-*k* dielectrics in order to investigate changes in materials properties. Despite the simplicity of the used models, the results captured a major difference between the 2.4 and 2.1 low-*k* generations. The porosity load in the latter ILD's will be above the percolation threshold, which impacts significantly its thermal and mechanical properties, and the materials compatibility with various production stages. By developing appropriate models for suitable representation of the porosity, a more accurate quantitative analysis can be achieved.

ACKNOWLEDGMENTS

The author would like to thank Dr. Patrick Smith for valuable comments. This research was carried out at the Jet Propulsion Laboratory, California Institute of Technology, under a contract with the National Aeronautics and Space Administration.

REFERENCES

1. L. Peters, *"Industry divides on low-k dielectric choices"*, Semiconductor International, May 2001.
2. Semiconductor Industry Association, *International Technology Roadmap for Semiconductors, 2001 Edition*, (http://public.itrs.net/Files/2001ITRS/Home.htm).
3. D. Stauffer and A. Aharony, *Introduction to Percolation Theory*, (Taylor and Francis, London, (1994).
4. M.B. Isichenko, Rev. Mod. Phys. **64**, 961 (1992); and references therein.
5. M. Sahimi, *Applications of Percolation Theory*, (Taylor & Francis, London, 1994).
6. N. Jan, Physica A **266**, 72 (1999).
7. H. Scher and R. Zallen, J. Chem. Phys. **53**, 3759 (1979).
8. J.D. Bernal, Nature **185**, 68 (1960).
9. M.J. Powell, Phys. Rev. B **21**, 3725 (1980).
10. M. Ahmadzadeh and A.W. Simpson, Phys. Rev. B **25**, 4633 (1982).
11. A.L.R. Bug, S.A. Safran, G.S. Crest, and I. Webman, Phys. Rev. Lett. **55**, 1896 (1985).
12. D.P. Bentz, E.J. Garboczi, and K.A. Snyder, *"A hard core/soft shell microstructural model for studying percolation and transport in three-dimensional composite media"*, NISTIR 6265, U.S. Department of Commerce, 1999.
13. *"IBM perfects new technique for making high-performance microchips"*, East Fishkill, NY, April 3, 2000 (Cu-11 process).
14. R.D. Miller, Reports on Dow/IBM NIST-ATP project 98-06-0052: *"Ultra-Low Dielectric Constant Materials for Integrated Circuit Interconnects"* (unpublished).
15. C.J. Hawker, J.L Hedrick, R.D. Miller, and W. Volksen, MRS Bulletin, April 2000, p. 54.